

# Unveiling the Potential of Diatomaceous Earth for the Synthesis of Sustainable Geopolymer Binders

R. S. Magalhães<sup>a\*</sup> , B. P. Bezerra<sup>a</sup>, M. R. Morelli<sup>b</sup>, A. P. Luz<sup>a,b</sup> 

<sup>a</sup>Universidade Federal de São Carlos, Rod. Washington Luiz, km 235, 13565-905, São Carlos, SP, Brasil.

<sup>b</sup>Universidade Federal de São Carlos, Departamento de Engenharia de Materiais, Rod. Washington Luiz, km 235, 13565-905, São Carlos, SP, Brasil.

Received: January 14, 2025; Revised: April 03, 2025; Accepted: May 15, 2025

This study explored the use of natural diatomaceous earth (ND) and brewery waste diatomaceous earth (BWD) as precursors for the synthesis of geopolymeric binders, with a focus on optimizing the developed compositions and analyzing their physico-mechanical and microstructural properties. Geopolymers were synthesized using various precursor combinations, with adjustments to their  $\text{SiO}_2/\text{Al}_2\text{O}_3$  molar ratios. ND exhibited high reactivity as a precursor, yielding compositions with compressive strengths of up to 28.59 MPa after 24 hours of curing and low porosity. This performance was attributed to the formation of an amorphous gel with a high density of Si–O–Si(Al) bonds. In contrast, systems incorporating BWD demonstrated reduced performance due to their elevated  $\text{SiO}_2/\text{Al}_2\text{O}_3$  molar ratio and limited geopolymerization, resulting in the presence of unreacted particles within the final microstructure. Stoichiometric adjustments and mechanical activation were critical in improving the compositions performance and enhancing the reactivity of the BWD residue, enabling the production of geopolymers with compressive strengths reaching 31.34 MPa. These findings emphasize the importance of optimizing both the chemical composition and synthesis processes to advance the development of geopolymeric materials, facilitating novel precursor combinations and the sustainable reutilization of industrial waste.

**Keywords:** *geopolymer, diatomite, metakaolin, binder, physico-mechanical properties.*

## 1. Introduction

Alkaline geopolymers are inorganic polymers synthesized at low temperatures ( $< 60^\circ\text{C}$ ) through the polycondensation of species formed by reactions between amorphous aluminosilicate sources and highly alkaline solutions, resulting in a rigid macromolecular matrix<sup>1</sup>. These materials are considered a sustainable alternative to conventional Portland cement due to their lower carbon footprint and ability to incorporate industrial waste and by-products, such as fly ash, blast furnace slag, rice husk ash, and sugarcane bagasse, among others<sup>2-4</sup>.

A geopolymer is a material composed of two key components: (i) an aluminosilicate-rich powder, referred to as the precursor, and (ii) an alkaline solution with a high pH (activating solution), which must be aqueous to ensure proper homogenization during the mixing stage<sup>5</sup>. Although both alkali-activated materials (AAM) and inorganic polymers (geopolymers) utilize an activating solution in their composition, they are fundamentally distinct. Ground granulated blast furnace slag is the most commonly used precursor for AAM due to its high calcium oxide (CaO) content. When exposed to alkaline solutions, it promotes the formation of hydrated products similar to calcium silicate hydrate (CSH), which contribute to the material's strength and durability. Conversely, geopolymers rely on precursors with high silica ( $\text{SiO}_2$ ) and alumina ( $\text{Al}_2\text{O}_3$ ) contents. When these precursors are combined with an

activating solution rich in potassium ( $\text{K}^+$ ) or sodium ( $\text{Na}^+$ ) ions, a series of reactions initiates the polycondensation process, leading to the formation of a three-dimensional polymeric network. As a result of these transformations, geopolymers exhibit an amorphous or semicrystalline structure with high mechanical strength, consisting entirely of inorganic elements<sup>6</sup>.

While various industrial, agro-industrial, and other waste by-products have been explored as aluminosilicates sources<sup>7-9</sup>, relatively few studies have investigated the use of natural or residual diatomaceous earth as a precursor in geopolymer formulations<sup>10-13</sup>. Nonetheless, this material is abundant, exhibits pozzolanic properties, and contains a high percentage of amorphous silica, making it a promising candidate for the development of novel geopolymer binders<sup>14,15</sup>.

Diatomaceous earth is commercially available in its natural form or as a by-product of certain industrial processes. For instance, in beer production, diatomite is used in the purification and clarification stages, but it has a limited lifespan due to the accumulation of organic compounds from the fermentation process. Once saturated, this material is no longer suitable for filtration, leading to the generation of up to 30 tons of waste per month in large breweries<sup>16</sup>. The annual production of brewery waste diatomite (BWD) is estimated at approximately 378,000 tons<sup>14</sup>. After the final filtration stage, this material is typically discarded in landfills, raising significant environmental concerns.

\*e-mail: [rmagalhaescaxias@gmail.com](mailto:rmagalhaescaxias@gmail.com)

Due to its low thermal conductivity, BWD can be utilized in brick production and other materials designed for thermal and acoustic insulation<sup>17,18</sup>. It can also partially replace cement in pozzolanic applications<sup>19-21</sup>. Additionally, this waste can be incorporated into geopolymer formulations, either as a precursor<sup>10</sup> or as an alternative silica source in the activating solutions<sup>11,12</sup>.

Garcia-Diaz<sup>10</sup> synthesized geopolymers incorporating 30 wt.% to 70 wt.% diatomite (from brewery filtration) into the formulations and systematically evaluated their properties after curing at room temperature and at 7, 28, and 56 days. The resulting pastes exhibited compressive strengths ranging from 13.7 MPa to 36.8 MPa. Notably, compositions with up to 60 wt.% of this waste showed increased apparent density while maintaining total porosity above 30%. Font<sup>11</sup> investigated four geopolymer systems, replacing sodium silicate with either commercial diatomite or BWD. After a 7-day curing period, the samples containing commercial diatomite or the industrial waste exhibited compressive strengths of 30.27 MPa and 29.06 MPa, respectively. Additionally, pre-treating BWD at 650°C for 1 hour enhanced its reactivity, leading to compositions with up to a 100% improvement in mechanical performance. Mejía<sup>12</sup> examined the incorporation of up to 45 wt.% brewery waste diatomite and rice husk ash (RHA) in the activating solution for geopolymer synthesis. The resulting paste exceeded 30 MPa in compressive strength after 7 days, outperforming formulations prepared with an RHA-based alkaline solution. Moreover, the compositions exhibited a water absorption of 26.77% and an apparent density of 1.32 g/cm<sup>3</sup>, highlighting their favorable physical properties.

The synthesis of geopolymers is highly dependent on the precursor material, its chemical composition, processing conditions, and precise stoichiometric adjustment of aluminosilicate-rich raw materials<sup>3,7</sup>. Optimizing these factors enhances precursor reactivity, phase formation, durability, and mechanical properties of the resulting geopolymers<sup>22,23</sup>. To fully explore the potential and broaden the applications of diatomaceous earth-based geopolymers, it is essential to understand how synthesis and processing parameters—such as calcination temperature, chemical composition, precursor type, activating solution, and curing conditions—affect both the setting kinetics of fresh mixtures and the final microstructure and mechanical properties of the solidified products<sup>3,10,14</sup>.

In this context, this study evaluated the physical, mechanical, and microstructural properties of geopolymers synthesized using natural diatomite (ND) and brewery waste diatomite (BWD, from a Brazilian beverage industry) as precursors. Various formulations were developed to maximize waste utilization, promote its reuse, and assess the impact of processing variables on the final properties of the geopolymer pastes.

2. Experimental Procedure

2.1. Materials and formulations

To prepare the geopolymers, the following materials were utilized:

- I. *Precursors* – commercial metakaolin ( $d_{50}$  = 34.0  $\mu$ m, Metakaolin HP Ultra, Metacaulim do Brazil), natural diatomite (ND,  $d_{50}$  = 10.0  $\mu$ m, Minasolo, Brazil), brewery waste diatomite (BWD,  $d_{50}$  = 20.0  $\mu$ m, AMBEV company, Brazil), and hydratable alumina ( $d_{50}$  = 6.0  $\mu$ m, Alphabond 300, Almatiss, Brazil). The chemical composition of these raw materials is shown in Table 1.
- II. *Alkaline solution* – prepared by mixing an aqueous sodium hydroxide solution (PA, Nox Lab Solutions, Brazil) with a concentration of 12M, and a colloidal silica suspension (SiO<sub>2</sub> = 40 wt.%, Levasil CS40-125, Nouryon, Brazil). The mixture was designed to achieve fixed molar ratios of SiO<sub>2</sub>/Na<sub>2</sub>O  $\approx$  1.5 and Na<sub>2</sub>O/H<sub>2</sub>O = 15<sup>24</sup>.

The diatomites (ND and BWD) were subjected to calcination at 800°C for 2 hours to enhance their reactivity and remove potential organic contaminants originating from the beer filtration process. However, despite this treatment, some peaks corresponding to quartz, muscovite, and cristobalite were still identified in the selected precursors, as shown in Figure 1.

Initially, both the individual and combined use of these materials with metakaolin were investigated (Tables 2 and 3), with the goal of determining which precursor combinations would yield pastes exhibiting optimal properties.

Table 1. Chemical composition (wt.%) of the raw materials evaluated in this study.

Raw materials	SiO <sub>2</sub>	Al <sub>2</sub> O <sub>3</sub>	Fe <sub>2</sub> O <sub>3</sub>	MgO	Na <sub>2</sub> O	K <sub>2</sub> O	Others	SiO <sub>2</sub> /Al <sub>2</sub> O <sub>3</sub> *	LOI** (%)
Metakaolin (MKHP)	55.58	39.40	1.95	0.65	-	0.56	1.86	2.39	0.12
Natural diatomite (ND)	53.68	40.03	0.83	0.46	0.06	4.15	0.79	2.28	0.41
Brewery waste diatomite (BWD)	90.95	4.64	2.12	0.09	0.74	0.40	1.06	33.32	0.98
Hydratable alumina (HA)	0.01	91.0	-	-	0.4	-	-	-	8.2

\* Molar ratio. \*\* Loss on ignition up to 1000 °C.

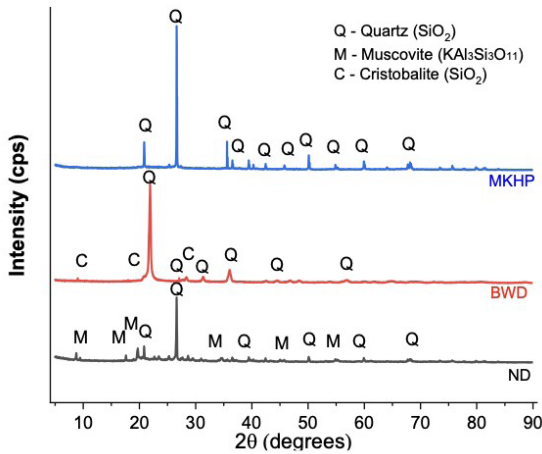


**Figure 1.** X-ray diffraction profiles of the selected precursors (MK-HP = metakaolin, BWD = brewery waste diatomite, and ND = natural diatomite). ND and BWD were calcined at 800°C for 2 hours.

Considering the chemical composition of BWD and the high  $\text{SiO}_2/\text{Al}_2\text{O}_3$  molar ratios in the formulations containing this material (Table 2), further stoichiometric adjustments were required for the geopolymer pastes. To standardize the compositions and facilitate a more precise comparison, a supplementary  $\text{Al}_2\text{O}_3$  source was incorporated into the formulations containing the selected waste. The precursor proportions were optimized using Solver tool in Excel (Microsoft), resulting in adjusted  $\text{SiO}_2/\text{Al}_2\text{O}_3$  ratios ranging from 2.5 to 4.0, as detailed in Table 3. Additionally, BWD underwent preliminary mechanical activation via ball milling at 30 rpm for 3 hours to improve its reactivity.

Building on the results, a third step focused on selecting the MBWD-HA2.5 formulation (hereafter referred to as BWD4) as the most promising geopolymer due to its superior mechanical performance. The Solver tool was then used again to develop new compositions aimed at maximizing the incorporation of diatomite waste while also incorporating metakaolin and hydratable alumina as

**Table 2.** Precursors used in the formulations of the geopolymeric pastes.

Compositions	Precursors (wt.%)			$\text{SiO}_2/\text{Al}_2\text{O}_3$ (molar ratio)
	Metakaolin - MKHP	Natural diatomite - ND	Brewery waste diatomite – BWD	
M100	100	-	-	2.97
ND25	75	25	-	2.94
ND50	50	50	-	2.91
ND75	25	75	-	2.87
ND100	-	100	-	2.84
BWD25	75	-	25	4.30
BWD50	50	-	50	6.68
BWD75	25	-	75	12.17
BWD100	-	-	100	38.20

**Table 3.** Additional formulations considering adjustments to the stoichiometry of the pastes containing brewery waste diatomite (BWD).

Compositions	Precursors (wt.%)			$\text{SiO}_2/\text{Al}_2\text{O}_3$ **	Liquid content (wt.%)***
	Metakaolin (MKHP)	Brewery waste diatomite (BWD)*	Hydratable alumina (HA)		
BWD-HA2.5	-	57.86	42.14	2.5	70 (LR)
BWD-HA3	-	62.94	37.06	3.0	70 (LR)
BWD-HA3.5	-	67.04	32.96	3.5	70 (LR) + 20 (water)
BWD-HA4	-	70.40	29.60	4.0	70 (LR) + 30 (water)
MBWD-HA2.5	86.10	3.97	9.93	2.5	70 (LR)
MBWD-HA3	82.88	10.98	6.14	3.0	70 (LR) + 10 (water)
MBWD-HA3.5	74.14	20.50	5.36	3.5	70 (LR) + 10 (water)
MBWD-HA4	66.23	28.78	4.99	4.0	70 (LR) + 10 (water)
BWD8	79.80	8.00	12.20	2.5	70 (LR)
BWD16	67.00	16.00	17.00	2.5	70 (LR)
BWD24	62.00	24.00	22.50	2.5	70 (LR) + 10 (water)
BWD32	41.30	32.00	26.70	2.5	70 (LR) + 20 (water)

\* The waste underwent a pre-activation process to enhance its reactivity, which involved grinding in a ball mill at 30 rpm for 3 hours. \*\* Molar ratio. \*\*\* LR = alkaline liquid reagent.

precursors. These geopolymers were designed to maintain a fixed  $\text{SiO}_2/\text{Al}_2\text{O}_3$  molar ratio of 2.5 (compositions labeled BWD8–BWD32, Table 3).

## 2.2. Synthesis and processing of the geopolymers

The precursors and activating solution, at a mass ratio of 1:0.7, were mixed in a planetary mixer (Solotest, Brazil) at low speed for 1 minute to incorporate the alkaline solution, followed by 5 minutes of mixing at high speed to produce a viscous paste. This paste was then molded under vibration to form cylindrical specimens (40 mm x 40 mm), which were covered with plastic film and cured in an oven at 40°C for 24 hours.

## 2.3. Characterization of the geopolymers

The following tests were conducted to characterize the geopolymer samples after the curing stage: (1) compressive strength, measured according to ASTM C133-97 using a universal testing machine (EMIC, DL10000); (2) water absorption, apparent porosity, and apparent density, determined based on the Archimedes principle with water as the immersion medium (ASTM C830-00).

Additionally, powder samples from the most promising compositions underwent further analysis using: 1) Fourier transform infrared spectroscopy (FTIR, PerkinElmer Spectrum 3) in the range of 4000–400  $\text{cm}^{-1}$ , with 20 scans and a resolution of 4  $\text{cm}^{-1}$ , using attenuated total reflectance (ATR); 2) X-ray diffraction (Bruker D8 Focus,  $\text{CuK}\alpha$  radiation [ $\lambda = 1.5418 \text{ \AA}$ ], nickel filter, 40 mA, 40 mV, and step size of 0.02°) to identify the structural properties of the precursors and synthesized geopolymers; and 3) scanning electron microscopy (Tescan MIRA, USA) combined with energy-dispersive X-ray spectroscopy (EDS) to examine the microstructure of fractured surfaces of the samples.

## 3. Results and Discussion

### 3.1. Geopolymer pastes formulated from metakaolin or a blend of metakaolin with natural diatomite or brewery waste diatomite

The geopolymers synthesized from natural diatomite (Figure 2a) exhibited excellent compressive strength,

ranging from 20.97 MPa to 28.59 MPa after 24 hours of curing at 40°C, with apparent porosity values between 7.62% and 5.97%. Notably, the ND75 and ND100 formulations outperformed the reference composition M100 (23.75 MPa), demonstrating the high potential of natural diatomite for applications requiring superior early-age mechanical strength. This aligns with previous studies indicating that the alkaline solution used in this research, particularly when combined with metakaolin, fosters sufficient reactivity to produce fast-setting geopolymers<sup>13,24,25</sup>.

In contrast, the compositions incorporating diatomaceous earth waste displayed lower mechanical strength (Figure 2b). Additionally, samples from the BWD100 formulation partially dissolved in water during porosity testing, suggesting ineffective geopolymerization under the evaluated conditions<sup>26</sup>. As indicated in Table 1, BWD has a high  $\text{SiO}_2$  content (> 90 wt.%), whereas metakaolin and ND contain 53–55 wt.% of this oxide. Generally, geopolymer systems with elevated  $\text{SiO}_2/\text{Al}_2\text{O}_3$  ratios (> 4) tend to exhibit reduced compressive strength. This behavior is attributed to an excess of inactive silica species in the reaction medium, which contributes to defect formation and increased porosity in the resulting specimens<sup>27,28</sup>.

X-ray diffraction revealed the presence of residual crystalline phases from the precursors, including cristobalite and quartz, within the geopolymer matrix. However, it is well established that these phases do not significantly contribute to geopolymerization<sup>12</sup>. Cristobalite was detected exclusively in compositions containing BWD, with its characteristic peak appearing around  $2\theta = 20^\circ$  (Figure 3). In contrast, geopolymers based on natural diatomite (ND) and metakaolin exhibited an amorphous matrix interspersed with residual crystalline phases (quartz and muscovite) originating from the precursors. Since the activating solutions used in this study contained dissolved reactive silica, the results suggest that the dissolution of aluminum species from metakaolin or calcined diatomite (ND) in a highly alkaline environment facilitated the geopolymerization process<sup>24,29</sup>, leading to the formation of an amorphous gel within the matrix of the samples.

Consistent with these findings, ATR-FTIR analysis of the BWD50 composition (Figure 4) revealed high-intensity bands at 1013  $\text{cm}^{-1}$ , corresponding to T-O-T bonds (where T = Si or Al),

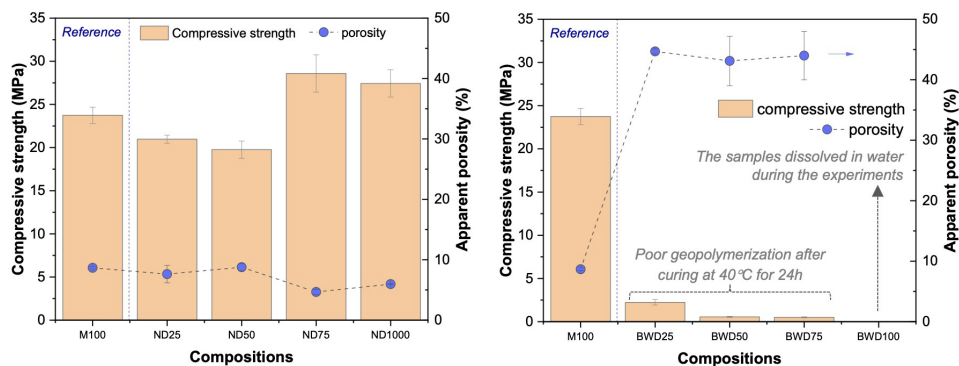


**Figure 2.** Compressive strength and apparent porosity of the geopolymer pastes prepared with metakaolin (M), or the blending of metakaolin with (a) natural diatomite (ND), or (b) brewery waste diatomite (BWD) as precursors. All samples were kept at 40°C for 24h before the measurements.

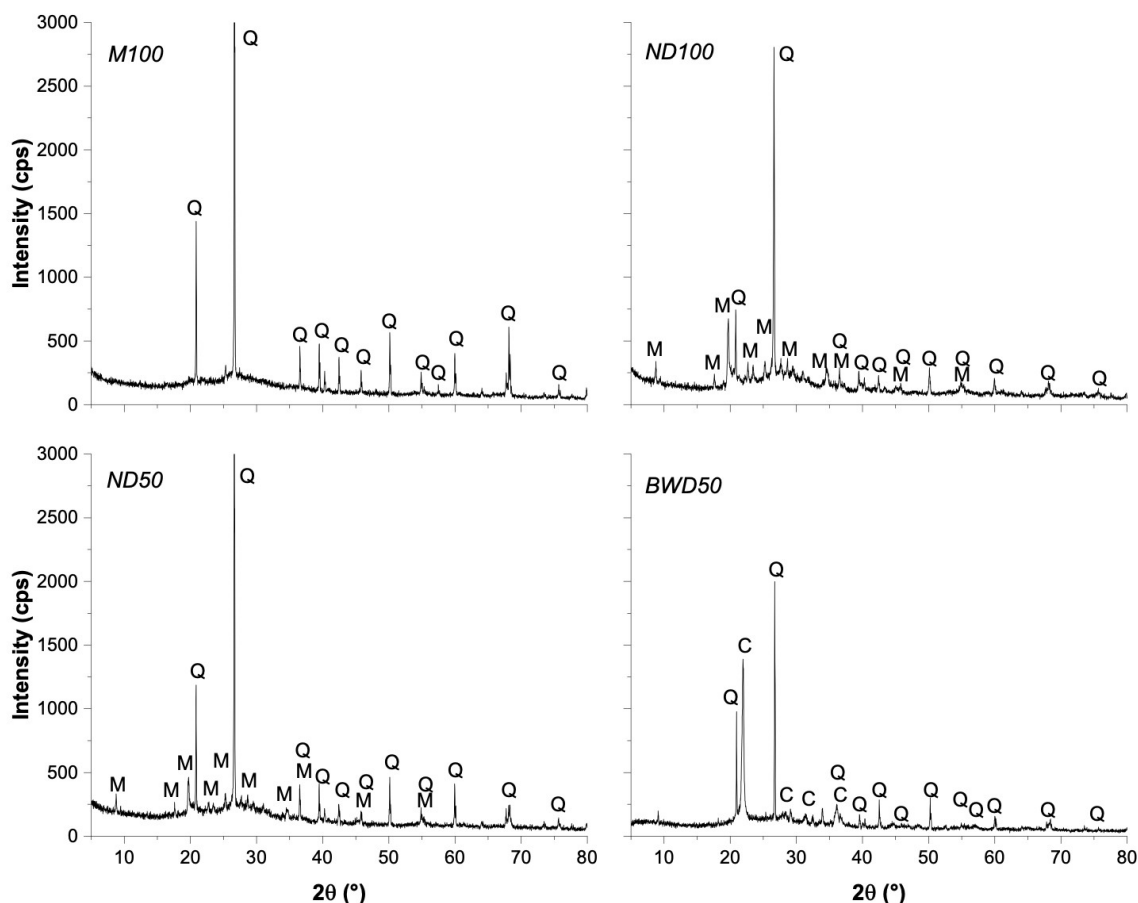


**Figure 3.** XRD profiles of the geopolymer pastes prepared with metakaolin (M100), natural diatomite (ND100), or the blending of 50 wt.% metakaolin + 50 wt.% natural diatomite (ND50) and 50 wt.% metakaolin + 50 wt.% brewery waste diatomite (BWD50) as precursors. All samples were kept at 40°C for 24h before the measurements. Q = a-quartz ( $\text{SiO}_2$ , 83-2465), M = muscovite ( $\text{KA}_1\text{Si}_3\text{O}_{11}$ , 46-741) and C = cristobalite ( $\text{SiO}_2$ , 77-1317).

and additional peaks in the 606 to 791  $\text{cm}^{-1}$  range, indicating the presence of unreacted particles that did not fully participate in the geopolymerization reaction<sup>30,31</sup>. Specifically, the band at 791  $\text{cm}^{-1}$  detected in both the residue (BWD, data not shown here) and geopolymer (BWD50, Figure 4) spectra is attributed to characteristic O-Si-O bending vibrations<sup>10</sup>.

The ND50 and ND100 pastes displayed a more defined and characteristic geopolymer spectrum (Figure 4), with primary bands around 971–967  $\text{cm}^{-1}$  (T-O-T bonds, where T = Si or Al), indicating a higher degree of geopolymerization in these systems compared to BWD50. This suggests a substantial presence of Si-O-Al and Si-O-Si bonds, which are key to the hardening and mechanical reinforcement of the samples, as previously reported<sup>31</sup>. Additionally, stretching and bending vibrational bands associated with O-H bonds were observed at 3380  $\text{cm}^{-1}$  and 1392  $\text{cm}^{-1}$ , respectively. These bands correspond to physically adsorbed water, moisture retained within microstructural voids, or unreacted hydroxylated silicate groups<sup>24</sup>. Furthermore,  $\text{CO}_3^{2-}$  species were identified at 1644  $\text{cm}^{-1}$ , suggesting the possible formation of alkaline carbonate compounds<sup>10</sup>.

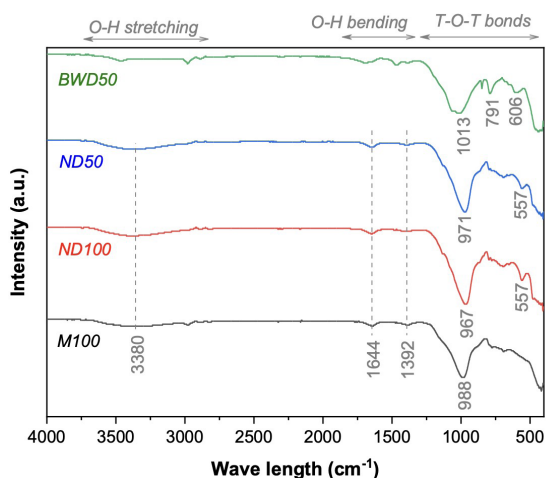


**Figure 4.** ATR-FTIR spectra of the geopolymer pastes prepared with metakaolin (M100), natural diatomite (ND100), or the blending of 50 wt.% metakaolin + 50 wt.% natural diatomite (ND50) and 50 wt.% metakaolin + 50 wt.% brewery waste diatomite (BWD50) as precursors. All samples were kept at 40°C for 24h before the measurements.



### 3.2. Adjustment of the stoichiometry of the pastes comprising diatomite waste as precursors

#### 3.2.1. Mixtures containing diatomite waste and hydratable alumina as precursors

Figure 5a highlights the critical role of chemical stoichiometry in the properties of geopolymers formulated with BWD and hydratable alumina. Importantly, the BWD-HA2.5 composition exhibited the most favorable results, achieving a compressive strength of 4.01 MPa and an apparent porosity of 13.22%.

Although the mechanical properties of the new formulations exceeded that of the compositions prepared exclusively with BWD (Figure 2b), the results remained significantly lower than those of the reference geopolymer (M100). Furthermore, the new formulations displayed increased water absorption (9.52–14.58%) and low apparent density (1.28–1.39 g/cm<sup>3</sup>, Figure 5b). These findings align with the FTIR spectra presented in Figure 6, which indicate that geopolymerization was not fully realized in the systems containing BWD and alumina. This is evidenced by the less intense and broader band observed near the wavelength of 1075-972 cm<sup>-1</sup>.

In addition to stoichiometric adjustments, the enhanced performance of these compositions can be attributed to the mechanical activation of the precursors. As reported in<sup>22</sup>, this grinding process increases surface area, alters crystalline structures, and enhances the material's reactivity by exposing active sites on raw material surfaces, thereby improving its suitability for geopolymerization. Consequently, geopolymers formulated exclusively with hydratable alumina and BWD also exhibited rapid hardening, which posed challenges during the specimens molding.

#### 3.2.2. Combining metakaolin with diatomite waste and hydratable alumina as precursors

Metakaolin was incorporated into the previously studied compositions, with adjustments made to maintain the selected molar ratios between 2.5 and 4.0 (Table 3). The physical and

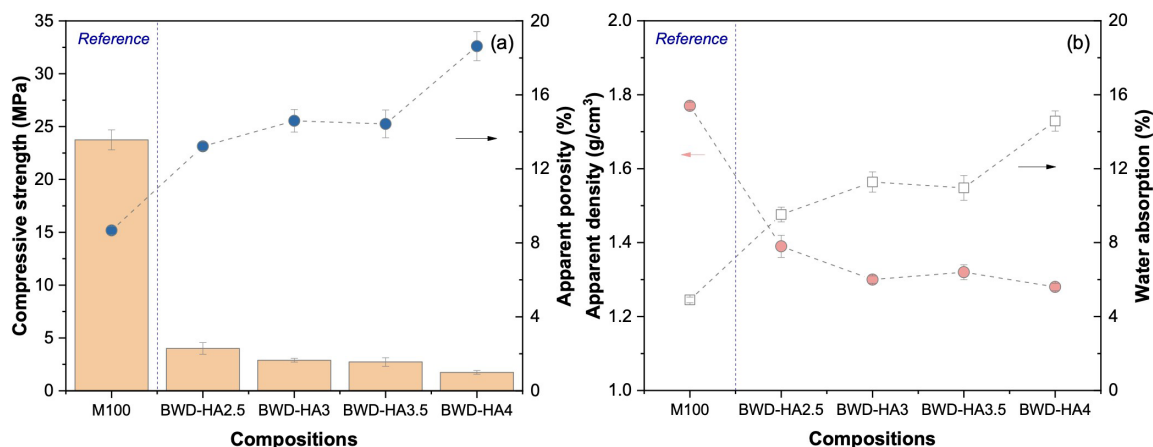
mechanical properties of these newly tested formulations are presented in Table 4.

The compressive strength of geopolymers prepared using diatomaceous earth as a precursor and reactive silica dissolved in an alkaline solution generally increases as the SiO<sub>2</sub>/Al<sub>2</sub>O<sub>3</sub> molar ratio decreases<sup>13</sup>. This trend is evident in Table 4, where the composition with a SiO<sub>2</sub>/Al<sub>2</sub>O<sub>3</sub> ratio of 2.5 demonstrates the highest mechanical performance. The developed pastes achieved compressive strengths ranging from 11.06 MPa for MBWD-HA4 to 22.40 MPa for MBWD-HA2.5. This improvement is attributed to the properties of the geopolymeric gel and the predominant presence of metakaolin in the formulation, which plays a key role in geopolymerization process and promotes the formation of isolated pores<sup>32</sup>. Consequently, these values are comparable to those of the reference composition (M100), with MBWD-HA2.5 exhibiting lower porosity (4.13% compared to 8.67%).

In the FTIR spectra, all compositions showed a well-defined band around 988 cm<sup>-1</sup>, particularly when comparing the data shown in Figure 6 and Figure 7. This suggests a more advanced geopolymerization process and the stronger Si-O bond formation<sup>33,34</sup>.

#### 3.2.3. Maximizing the amount of waste to be incorporated into the geopolymer pastes

To optimize the incorporation of BWD into the developed compositions, new formulations were evaluated while maintaining the precursor stoichiometry at SiO<sub>2</sub>/Al<sub>2</sub>O<sub>3</sub> = 2.5. The waste content was varied between 4 wt.% and 32 wt.% in the new geopolymers (Table 3). As shown in Figure 8, an optimal BWD content enhances both physical and mechanical properties. The BWD8 composition demonstrated a compressive strength of approximately 31.34 MPa after 24 hours, with low porosity (5.17%) and a density of 1.79 g/cm<sup>3</sup>. Similarities in the XRD profiles and FTIR spectra of BWD4, BWD8, and BWD16 samples suggest that the mineralogical composition remained stable, and the added waste did not significantly alter the structure of the geopolymeric gel (Figure 9).

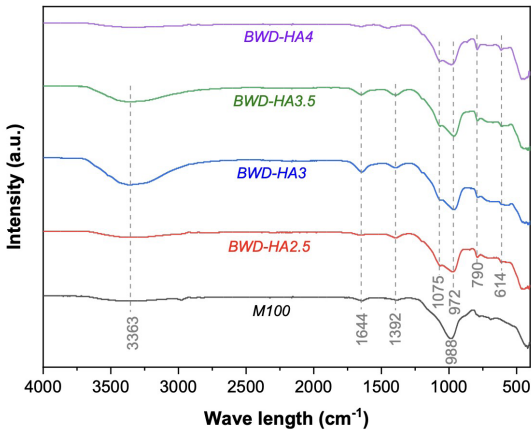
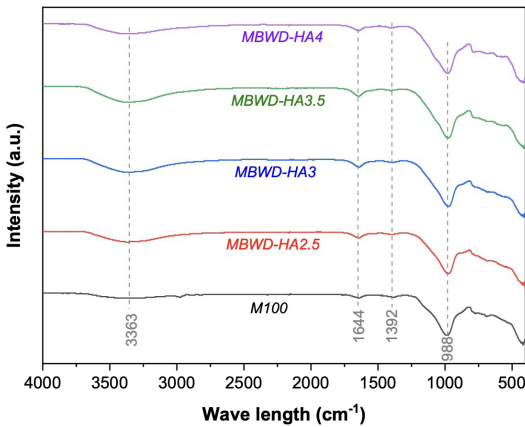


**Figure 5.** (a) Compressive strength and apparent porosity, and (b) apparent density and water absorption of the geopolymer pastes prepared with metakaolin (M) or brewery waste diatomite (BWD) + hydratable alumina (HA) as precursors. All samples were kept at 40°C for 24h before the measurements.

**Table 4.** Properties of the cured pastes (40°C for 24h) prepared with metakaolin (M) or the combination of metakaolin + brewery waste diatomite (BWD) + hydratable alumina (HA) as precursors.

Compositions	Compressive strength (MPa)	Apparent porosity (%)	Water absorption (%)	Apparent density (g/cm <sup>3</sup> )
M100*	23.75 ± 0.94	8.67 ± 0.22	4.09 ± 0.15	1.77 ± 0.01
MBWD-HA2.5	22.40 ± 1.64	4.13 ± 0.17	2.32 ± 0.09	1.78 ± 0.01
MBWD-HA3	18.89 ± 1.67	4.24 ± 0.55	2.40 ± 0.31	1.77 ± 0.01
MBWD-HA3.5	10.46 ± 0.38	4.34 ± 0.17	2.53 ± 0.11	1.72 ± 0.01
MBWD-HA4	11.06 ± 0.38	5.04 ± 0.51	2.97 ± 0.31	1.70 ± 0.01

\*Reference composition containing only metakaolin as precursor.

**Figure 6.** ATR-FTIR spectra of the geopolymer pastes prepared with metakaolin (M100) or brewery waste diatomite (BWD) + hydratable alumina (HA) as precursors. All samples were kept at 40°C for 24h before the measurements.**Figure 7.** ATR-FTIR spectra of the geopolymer pastes prepared with metakaolin (M100) or metakaolin + brewery waste diatomite (BWD) + hydratable alumina (HA) as precursors. All samples were kept at 40°C for 24h before the measurements.

The BWD16 composition presented compressive strength values comparable to the reference geopolymer (M100), indicating that residue content can be significantly increased without compromising mechanical performance. This also

resulted in samples with lower porosity (Figure 8b). However, incorporating residue contents of 24 wt.% or higher led to a decline in mechanical strength (Figure 8a), as an excessive residue amount may hinder the geopolymerization process and disrupt the formation of a more homogeneous matrix.

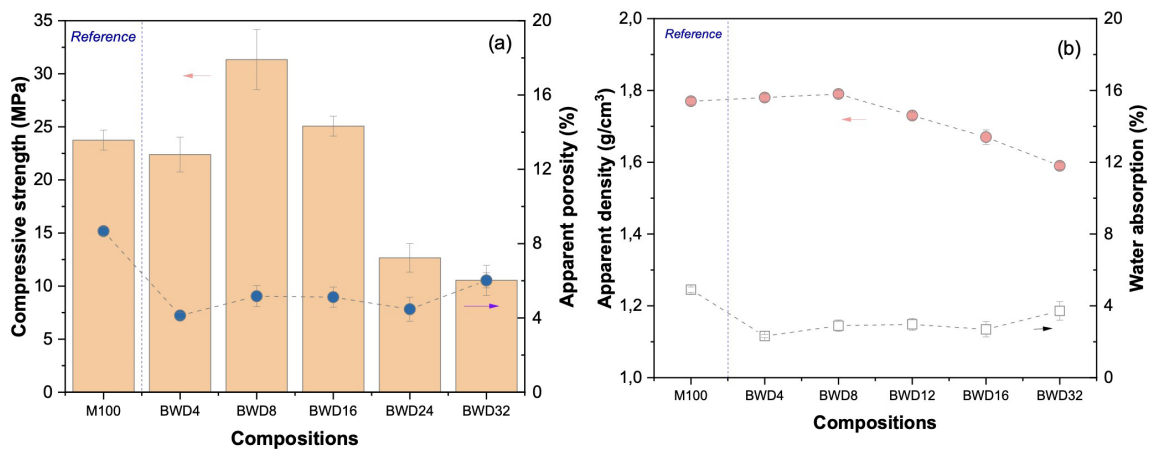
### 3.3. SEM-EDS analysis of the cured samples

Figure 10 shows the microstructure of fractured regions of geopolymeric pastes cured at 40°C. The M100 composition exhibited a homogeneous microstructure, with microcracks surrounding unreacted metakaolin particles (Point A, Figure 10a). Additionally, the matrix of the reference formulation consisted of an amorphous gel primarily composed of Si, Al, Na, and O (Point B, Table 5), corroborating the previously reported FTIR and XRD spectra (Figures 3 and 4).

The sample containing commercial diatomite (ND100, Figures 9c and 9d) showed particles characteristic of this mineral, with approximately 10 µm in size, which were uniformly distributed throughout the microstructure and retaining the characteristic frustule morphology (hollow and porous shells)<sup>19</sup>. EDS analysis of the ND100 paste (Points C and D in Figure 10 and Table 5) indicated a predominance of O, Al, Si, and Na in various regions of the sample. Additionally, small amounts of K and Fe were more prominently identified in the diatomite particles (Point C, Figure 10d), aligning with the chemical composition of this raw material (Figure 2).

In contrast, geopolymers containing BWD exhibited surfaces with a higher prevalence of microcracks and unreacted particles of the waste (Figures 10e and 10g). Cristobalite particles (SiO<sub>2</sub>, Point G in Figure 10f) were identified throughout the microstructure of the BWD8 composition. Partially dissolved alumina particles (Point E, Figure 10e), surrounded by microcracks, contributed to structural defects in the resulting microstructure. The area corresponding to Point F (Figure 10e) likely represents the gel phase, characterized by concentrations of Si, Al, and Na, confirming the formation of an amorphous geopolymeric matrix.

The EDS spectrum at Point H (Figure 10g and Table 5) reveals a high Si/Al molar ratio, indicative of a residual BWD particle. Correspondingly, scanning electron microscopy (SEM) images highlight the incomplete dissolution of BWD. This finding underscores the existence of a threshold for incorporating BWD into geopolymeric formulations. Excessive waste content disrupts gel formation<sup>12</sup>, which



**Figure 8.** (a) Compressive strength and apparent porosity, and (b) apparent density and water absorption of the geopolymer pastes prepared with metakaolin (M) or the blending of metakaolin + brewery waste diatomite (BWD) + hydratable alumina (HA) as precursors. The compositions containing distinct waste powder contents presented fixed  $\text{SiO}_2/\text{Al}_2\text{O}_3$  molar ratio = 2.5. All samples were kept at 40°C for 24h before the measurements.

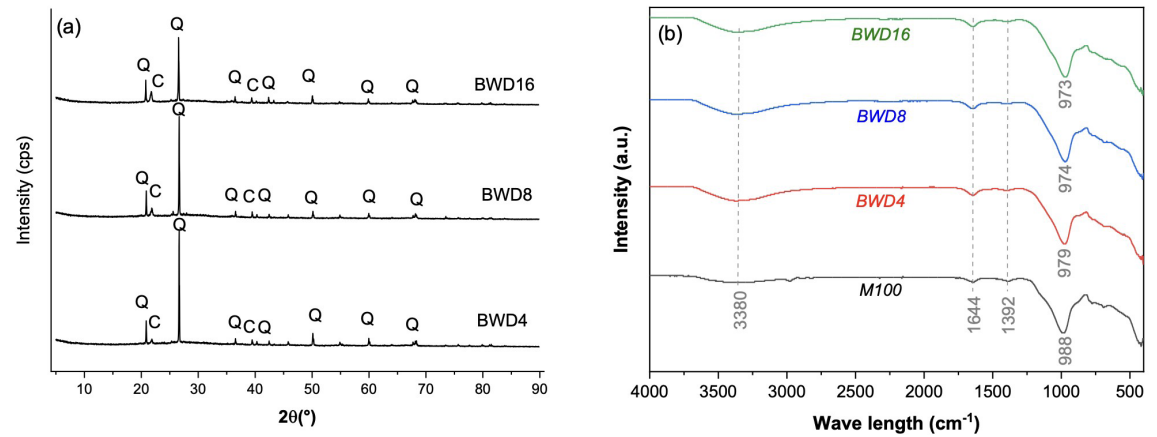


**Figure 9.** (a) XRD profiles and (b) ATR-FTIR spectra of the geopolymer pastes prepared with metakaolin (M) or the blending of metakaolin + brewery waste diatomite (BWD) + hydratable alumina (HA) as precursors. The compositions containing distinct waste powder contents presented fixed  $\text{SiO}_2/\text{Al}_2\text{O}_3$  molar ratio = 2.5. All samples were kept at 40°C for 24h before the measurements. Q =  $\alpha$ -quartz ( $\text{SiO}_2$ , 83-2465) and C = cristobalite ( $\text{SiO}_2$ , 77-1317).

**Table 5.** Chemical composition (EDS analysis) of the phases identified within the microstructure of the cured geopolymeric samples. The specific points corresponding to the analysis are marked in the images presented in Figure 9.

Samples	Mass (%)					
	Si	Al	Na	O	K	Fe
M100 (A)	31.09	14.88	9.85	39.95	-	2.50
M100 (B)	33.10	13.86	10.69	40.10	-	1.50
ND100 (C)	27.36	20.17	5.18	39.08	7.04	1.17
ND100 (D)	31.06	19.10	9.73	52.19	-	0.30
BWD8 (E)	11.96	40.38	8.02	39.64	-	-
BWD8 (F)	25.09	18.99	8.24	46.21	-	1.47
BWD8 (G)	59.11	-	-	40.89	-	-
BWD16 (H)	47.51	4.31	3.07	45.11	-	-
BWD16 (I)	35.30	16.07	11.48	35.87	-	1.27



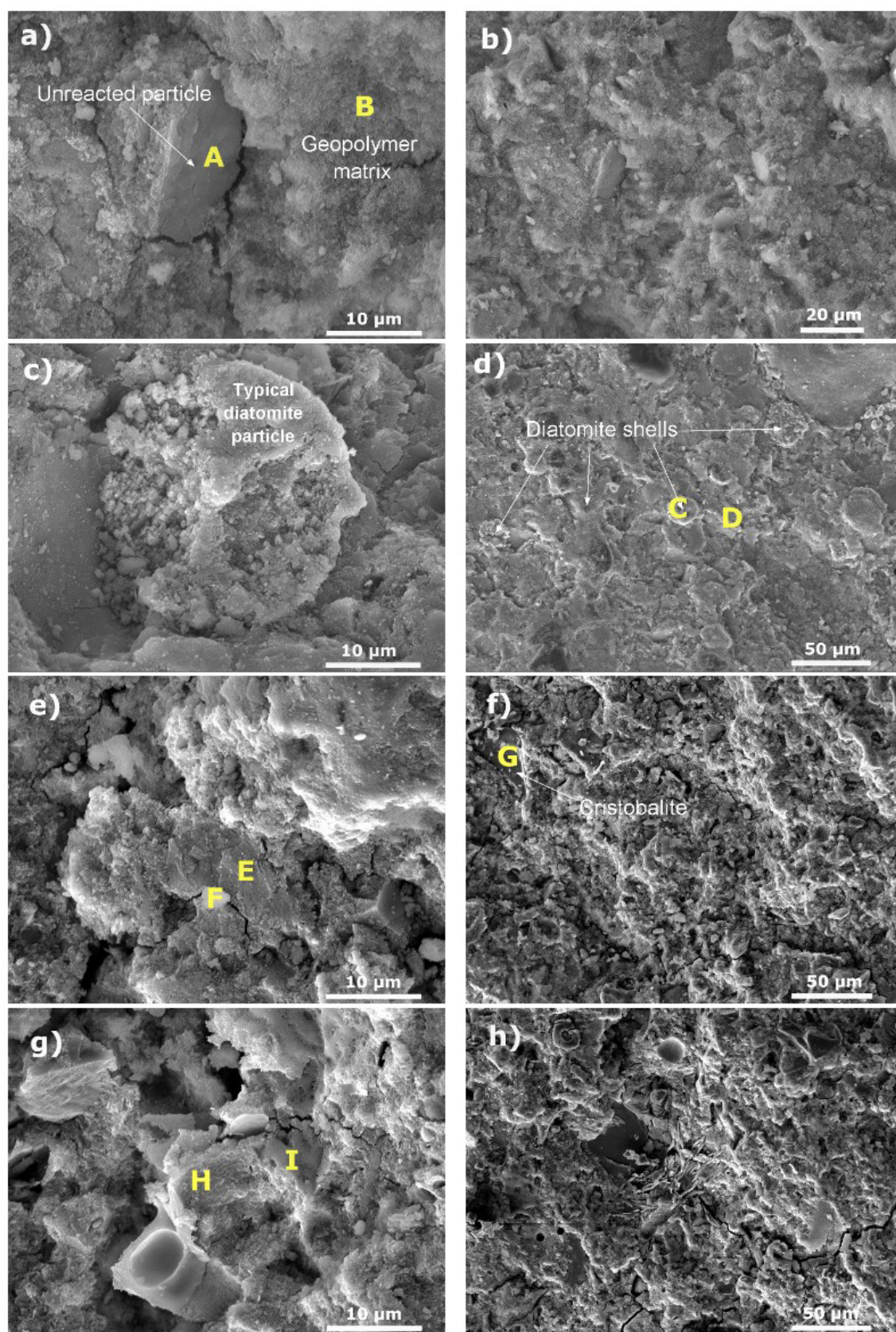


**Figure 10.** SEM images of the geopolymers: (a)-(b) M100, (c)-(d) ND100, (e)-(f) BWD8, and (g)-(h) BWD16. All samples were cured at 40°C for 24h before the measurements.

in turn increases porosity and diminishes the mechanical properties of the resulting ceramics. Point I (Figure 10g) represents a partially dissolved BWD particle, with the surrounding regions exhibiting noticeable microcracks. These microstructural features indicate limited interaction between the BWD particles and the geopolymeric matrix, further underscoring the challenges associated with excessive waste incorporation into the evaluated pastes.

## 4. Conclusions

This study investigated the synthesis and evaluation of geopolymeric binders incorporating diatomaceous earth as a precursor. The key findings derived from the results are as follows:

- The incorporation of natural diatomite (ND) as precursor led to the formation of geopolymers exhibiting compressive strengths greater than 30 MPa after curing at 40°C for 24 hours. These results highlight the potential of ND as effective precursor to produce geopolymeric binders with satisfactory early-age strength.
- Analysis by scanning electron microscopy (SEM), X-ray diffraction (XRD), and Fourier-transform infrared spectroscopy (FTIR) revealed that the incomplete dissolution of BWD significantly affected the density of Si–O–Si (Al) bonds in the geopolymeric pastes. This, in turn, influenced gel formation and, subsequently, the porosity and overall properties of the samples.
- Stoichiometric optimization of the waste-containing formulations, in combination with the mechanical activation of BWD, was crucial for promoting geopolymerization and enhancing the reactivity of the compositions. These approaches facilitated improvements in the mechanical and physical properties of the resulting geopolymers. Formulations exhibiting a  $\text{SiO}_2/\text{Al}_2\text{O}_3$  ratio of 2.5 demonstrated superior performance.
- The BWD8 formulation outperformed the reference composition (M100), achieving a compressive strength of 31.34 MPa after 24 hours, along with reduced porosity and increased density. However, increasing the BWD content above 24 wt.% resulted in a decline in mechanical strength, suggesting that an excess of this residue impairs the efficiency of the geopolymerization process and introduces defects into the microstructure.

These findings underscore the necessity of optimizing both the chemical composition and synthesis procedure to facilitate the development of advanced geopolymers, enabling novel combinations of precursors and the sustainable reuse of industrial waste materials.

## 5. Acknowledgments

This study was financed in part by the Coordenação de Aperfeiçoamento de Pessoal de Nível Superior - Brasil (CAPES) - Finance Code 001. This work was carried out with the support of Conselho Nacional de Desenvolvimento Científico e Tecnológico, CNPq (Processo 304005/2023-1). The

authors would like to thank Nouryon (Brazil) for supplying the colloidal silica used in this work. The authors are also grateful to Prof. Dr. Oscar Peitl and LaMaV (Vitreo Materials Laboratory, DEMa-UFSCar) for the FTIR analyses performed in this study.

## 6. References

1. Tome S, Nana A, Tchakouté HK, Temuujin J, Rüschler CH. Mineralogical evolution of raw materials transformed to geopolymer materials: a review. *Ceram Int.* 2024;50(19):35855-68. <http://doi.org/10.1016/j.ceramint.2024.07.024>.
2. Pobłocki K, Pawlak M, Drzeżdżon J, Gawdzik B, Jacewicz D. Clean production of geopolymers as an opportunity for sustainable development of the construction industry. *Sci Total Environ.* 2024;928:172579. <http://doi.org/10.1016/j.scitotenv.2024.172579>.
3. Jiang T, Liu Z, Tian X, Wu J, Wang L. Review on the impact of metakaolin-based geopolymer's reaction chemistry, nanostructure and factors on its properties. *Constr Build Mater.* 2024;412:134760. <http://doi.org/10.1016/j.conbuildmat.2023.134760>.
4. Zhao J, Tong L, Li B, Chen T, Wang C, Yang G, et al. Eco-friendly geopolymer materials: A review of performance improvement, potential application and sustainability assessment. *J Clean Prod.* 2021;307:127085. <http://doi.org/10.1016/j.jclepro.2021.127085>.
5. Longhi MA. Álcali-ativação de lodo de caulim calcinado e cinza pesada com ativadores convencionais e silicato de sódio alternativo [dissertation]. Porto Alegre: Universidade Federal do Rio Grande do Sul; 2015.
6. Palomo A, Grutzeck MW, Blanco MT. Alkali-activated fly ashes: a cement for the future. *Cement Concr Res.* 1999;29(8):1323-9. [http://doi.org/10.1016/S0008-8846\(98\)00243-9](http://doi.org/10.1016/S0008-8846(98)00243-9).
7. Sgarlata C, Vaccari FE, Formia A, Ferrari F, Leonelli C. Statistical significance of curing variables on geopolymerization of mining by-product untreated clay. *Appl Clay Sci.* 2024;250:107284. <http://doi.org/10.1016/j.clay.2024.107284>.
8. Santos A, Andrejkovičová S, Perná I, Almeida F, Rocha F. Mechanical and thermal properties of geopolymers derived from metakaolin with iron mine waste. *Appl Clay Sci.* 2024;258:107452. <http://doi.org/10.1016/j.clay.2024.107452>.
9. Hamcumpai K, Nuaklong P, Chindasiriphan P, Jongvivatsakul P, Tangaramvong S, Di Samo L, et al. High-strength steel fibre-reinforced geopolymer concrete utilising recycled granite waste and rice husk ash. *Constr Build Mater.* 2024;433:136693. <http://doi.org/10.1016/j.conbuildmat.2024.136693>.
10. García-Díaz A, Bueno-Rodríguez S, Felipe-Sesé MA, Eliche-Quesada D. Effect of the incorporation of spent diatomaceous earths on the properties of alkaline activation cements based on sewage sludge ash. *Arch Civ Mech Eng.* 2024;24:62. <http://doi.org/10.1007/s43452-024-00873-1>.
11. Font A, Soriano L, Reig L, Tashima MM, Borrachero MV, Monzó J, et al. Use of residual diatomaceous earth as a silica source in geopolymer production. *Mater Lett.* 2018;223:10-3. <http://doi.org/10.1016/j.matlet.2018.04.010>.
12. Mejía JM, Mejía De Gutiérrez R, Montes C. Rice husk ash and spent diatomaceous earth as a source of silica to fabricate a geopolymeric binary binder. *J Clean Prod.* 2016;118:133-9. <http://doi.org/10.1016/j.jclepro.2016.01.057>.
13. Coelho TPP, Bezerra BP, Verza JR, Luz AP, Morelli MR. Physico-mechanical properties of metakaolin and diatomite-based geopolymers. *Mater Lett.* 2023;349:134784. <http://doi.org/10.1016/j.matlet.2023.134784>.
14. Kipsanai JJ, Wambua PM, Namango SS, Amziane S. A Review on the incorporation of diatomaceous earth as a geopolymer-based concrete building resource. *Materials.* 2022;15(20):7130. <http://doi.org/10.3390/ma15207130>.



15. Bağcı C, Kutyla GP, Kriven WM. Fully reacted high strength geopolymer made with diatomite as a fumed silica alternative. *Ceram Int*. 2017;43(17):14784-90. <http://doi.org/10.1016/j.ceramint.2017.07.222>.
16. Goulart MR, Silveira CB, Campos ML, Almeida JA, Manfredi-Coimbra S, Oliveira AF. Metodologias para reutilização do resíduo de terra diatomácea proveniente da filtração e clarificação da cerveja. *Quim Nova*. 2011;34(4):625-9. <http://doi.org/10.1590/S0100-40422011000400014>.
17. Mateo S, Cuevas M, La Rubia MD, Eliche-Quesada D. Preliminary study of the use of spent diatomaceous earth from the brewing industry in clay matrix bricks. *Adv Appl Ceramics*. 2017;116(2):77-84. <http://doi.org/10.1080/17436753.2016.1221019>.
18. Kaplan G, Yavuz Bayraktar O, Bayrak B, Celebi O, Bodur B, Oz A, et al. Physico-mechanical, thermal insulation and resistance characteristics of diatomite and attapulgite based geopolymer foam concrete: effect of different curing regimes. *Constr Build Mater*. 2023;373:130850. <http://doi.org/10.1016/j.conbuildmat.2023.130850>.
19. Ferreira RLS, Pinto L, Nóbrega AF, Carneiro AMP. Diatomaceous earth: a review of its characteristics and effects on the properties of mortars. *Constr Build Mater*. 2024;421:135711. <http://doi.org/10.1016/j.conbuildmat.2024.135711>.
20. Letelier V, Tarela E, Muñoz P, Moriconi G. Assessment of the mechanical properties of a concrete made by reusing both: brewery spent diatomite and recycled aggregates. *Constr Build Mater*. 2016;114:492-8. <http://doi.org/10.1016/j.conbuildmat.2016.03.177>.
21. Arbi K, Palomo A, Fernández-Jiménez A. Alkali-activated blends of calcium aluminate cement and slag/diatomite. *Ceram Int*. 2013;39(8):9237-45. <http://doi.org/10.1016/j.ceramint.2013.05.031>.
22. Madirisha MM, Dada OR, Ikotun BD. Chemical fundamentals of geopolymers in sustainable construction. *Mater Today Sustain*. 2024;27:100842. <http://doi.org/10.1016/j.mtsust.2024.100842>.
23. Jiang T, Liu Z, Tian X, Wu J, Wang L. Review on the impact of metakaolin-based geopolymer's reaction chemistry, nanostructure and factors on its properties. *Constr Build Mater*. 2024;412:134760. <http://doi.org/10.1016/j.conbuildmat.2023.134760>.
24. Bezerra BP, Morelli MR, Luz AP. Effect of reactive silica sources on the properties of Na-metakaolin-based geopolymer binder. *Constr Build Mater*. 2023;364:129989. <http://doi.org/10.1016/j.conbuildmat.2022.129989>.
25. Hassan HS, Abdel-Gawwad HA, Vázquez-García SR, Israde-Alcántara I, Flores-Ramírez N, Rico JL, et al. Cleaner production of one-part white geopolymer cement using pre-treated wood biomass ash and diatomite. *J Clean Prod*. 2019;209:1420-8. <http://doi.org/10.1016/j.jclepro.2018.11.137>.
26. Bezerra BP, Soares GA, Morelli MR, Luz AP. Recycling of roof tile waste in the manufacturing of high-temperature metakaolin-based geopolymer composites. *Ceramica*. 2023;69(391):242-7. <http://doi.org/10.1590/0366-69132023693913528>.
27. Autef A, Joussein E, Gasgnier G, Rossignol S. Role of the silica source on the geopolymerization rate ALL or. *J Non-Cryst Solids*. 2012;358(21):2886-93. <http://doi.org/10.1016/j.jnoncrsol.2012.07.015>.
28. Duxson P, Mallicoat SW, Lukey GC, Kriven WM, van Deventer JSJ. The effect of alkali and Si/Al ratio on the development of mechanical properties of metakaolin-based geopolymers. *Colloids Surf A Physicochem Eng Asp*. 2007;292(1):8-20. <http://doi.org/10.1016/j.colsurfa.2006.05.044>.
29. Bezerra BP, Luz AP. High-alumina refractory castables bonded with metakaolin-based geopolymers prepared with different alkaline liquid reagents. *Ceram Int*. 2024;50(11):18628-37. <http://doi.org/10.1016/j.ceramint.2024.02.351>.
30. Chen W, Dong B, Peng K-D, Yang Q, Wang Y, Hong S. Optimization of microstructure and mechanical performance of clay-rich sand-washing slurry-based geopolymers. *Appl Clay Sci*. 2024;260:107551. <http://doi.org/10.1016/j.clay.2024.107551>.
31. Zhang J, Fu Y, Wang A, Dong B. Research on the mechanical properties and microstructure of fly ash-based geopolymers modified by molybdenum tailings. *Constr Build Mater*. 2023;385:131530. <http://doi.org/10.1016/j.conbuildmat.2023.131530>.
32. Song L, Lei W, Zhu X, Luo L, Wang Q. Microstructural and mechanical properties of high-strength geopolymer based on Martian soil simulant. *Vacuum*. 2024;230:113753. <http://doi.org/10.1016/j.vacuum.2024.113753>.
33. Bezerra BP, Luz AP. Novel alkaline solid reagent for the preparation of one-part metakaolin-based geopolymers. *Mater Lett*. 2024;363:136270. <http://doi.org/10.1016/j.matlet.2024.136270>.
34. Caciatori RA, Dal-Bó AG, Bernardin AM. Effect of Na<sup>+</sup> alkaline activation on the geopolymerization of a pure metakaolin at room temperature. *Miner Eng*. 2024;219:109068. <http://doi.org/10.1016/j.mineng.2024.109068>.